

Obstacle-Induced Shape Transformations of Granular Arches in a 3D Silo

Abhijit Sinha^{1,*}, Narayanan Menon^{2,**}, and Shankar Ghosh^{1,***}

¹Tata Institute of Fundamental Research, Mumbai. Homi Bhabha Road, Mumbai 400-005, India.

²Department of Physics, University of Massachusetts Amherst, MA 01003, USA.

Abstract. The formation of stable arches leads to intermittent clogging during discharge from hoppers. In recent work (Sinha et al. [1]) we have shown that a slender rod inserted into the flow can suppress clogging, with purely geometric considerations determining the optimal height of a rod for a given diameter. Building on that work, we now analyze the geometry of the arch through imaging, and find direct evidence that the rod participates in the clogging arch when optimally located. The rod modifies the shape of the arch, making it both asymmetric and variable in position. The shape of the arch also signals the best choice of rod diameter to minimize clogging.

1 Introduction

The controlled flow of grains through narrow outlets is a fundamental process in industries handling bulk materials, where predictable discharge is essential for productivity and reliability. However, when the outlet size becomes comparable to the diameter of the particles, the system becomes prone to clogging, where the flow unpredictably ceases ([5],[6]) due to self-supporting arches spontaneously formed by particles near the outlet [4]. Visually, during a jam, the arch manifests itself as a stable interface between the bulk B and the air.

Many studies ([3],[7]) have shown that strategically placing an obstacle near the outlet can effectively suppress clogging in 2-dimensional hoppers. In recent work (Sinha et al. [1]), we have shown that clogs are suppressed in the practically important 3D case, with strong suppression of clogging even with a slender rod. The optimal position of the obstacle is determined by geometry: clogging is most suppressed when arches form near the rod tip.

The paper aims to study how an obstacle affects the projected shape of the 2D surface onto a 1D interface ∂B (Fig. 1d). In this work, we show that the presence of the rod strongly affects not just the probability of arch-formation, but also the shape of the resultant arch. As the rod diameter increases, arches form farther from the outlet. When the rod is at or below the optimal location, it actively participates in the clogging, leading to the formation of asymmetric arches that are distinctly different from the symmetric shape of the unperturbed arch. The interface takes on a symmetric shape (∂B is normal to the rod) when it is primarily supported by the inner walls of the hopper, whereas asymmetry arises when the rod plays a significant load-bearing role.

2 Experiment Setup:

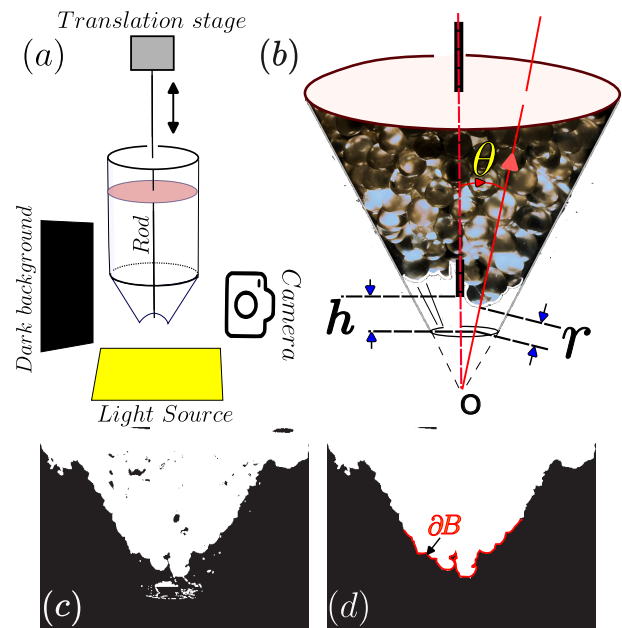


Figure 1. (a) Setup of the experiment. (b) A representative image of a clog, defining $r - \theta$ coordinates to parametrize the projected 2D shape of the arch. (c) The image after applying a smoothing filter, followed by a binary mask. (d) The lower boundary of the connected cluster (red curve) defines the 2D arch-shape.

The hopper (as shown in Fig. 1(a)) has a cylindrical upper section that ends in a conical funnel of 60° cut off at an outlet with a diameter of $a = 8$ mm. Spherical glass beads with a diameter of $d = 2.75 \pm 0.25$ mm, fill the hopper resulting in an opening-to-particle diameter ratio of approximately $a/d = 2.9$. Frequent clogging is observed within this parameter regime. For the obstacle we use long cylindrical carbon rods with three different diameters: 0.6,

*e-mail: abhijitsinha28@gmail.com

**e-mail: menon@physics.umass.edu

***e-mail: toshankarghosh@gmail.com

1.5, and 3.0 mm. The rod is centered along the axis of the hopper, with one end fixed to a motorized stage and the other end at height h from the opening. The motorized translation stage moves the rod tip at a speed of 5 mm/s from $h = 0$ (at the funnel opening) to the desired height h and then holds its position for a duration of $t = 10$ seconds before returning to the initial position. The duration t is chosen such that the system clogs during this period. 100–250 images of clogs are taken at each value of h with a USB-Teledyne Lumenera camera (resolution-1280×960). We choose values of h both above and below the optimal height $h = h_{pk}$ where the maximal suppression in clogging is observed. [1] The lighting and background (Fig. 1(a)) are adjusted to minimize reflections and enhance contrast.

2.1 Image analysis:

The image I (Fig. 1(b)) is first converted to grayscale. A mean filter with a neighborhood size of 4 pixels is applied to reduce noise and smoothen the image. The smoothed image is thresholded to create a binary mask, highlighting the main features. Interior holes in the binary image are filled (Fig. 1(c)). In the next step, we identify connected components in the binary image. The largest connected component B of the binary image is retained, while all smaller components are removed, effectively isolating the primary structure of interest (Fig. 1(d)). Finally, at every angle θ , (see Fig. 1(b)) we find the radial distance ρ of the boundary ∂B of the connected component, B . We measure $r(\theta) = \rho - \rho_{opening}$ (see Fig. 1(b)) to obtain the required interface.

3 Observations:

We present data for the shape of the projected arch for three rod diameters, each at heights above and below the the optimal location h_{pk} . The rod with $D = 1.5$ mm produces the best suppression of clogging. The statement is based on the mass flow experiments reported on the same system in the paper [1]

- **Arches include the rod only when above the optimal height.** We measure the projected shape of the arch ∂B and compute the mean height of the arch averaged over $\theta \in [-30^\circ, 30^\circ]$, denoted by $\langle r \rangle_\theta$. We plot $\langle r \rangle_\theta$ as a function of height h for different rod diameters D in Fig. 2(a). A sharp drop in $\langle r \rangle_\theta$ occurs beyond the optimal height h_{pk} where the clogging suppression is maximal [1], indicating that arches localize near the opening beyond this point. Furthermore, the error bars, which indicate variability in arch location, are much larger for $h < h_{pk}$, that is, when the rod is part of the arch-forming structure. In fact for values of $h > h_{pk}$ the standard error associated with the mean value of the $\langle r \rangle_\theta \rightarrow 0$ (see Fig. 2(a)). For rods with larger D , $\langle r \rangle_{\theta|h=h_c}$ registers a higher value, suggesting a flatter interface (see Fig. 2(a)).
- **Arches that include the rod are more asymmetric.** An example of this is shown in Fig. 2 (b). To quantify the asymmetry, we compute $\langle |r(L) - r(R)| \rangle$. Here, L and R denote the leftmost and rightmost extreme angles of

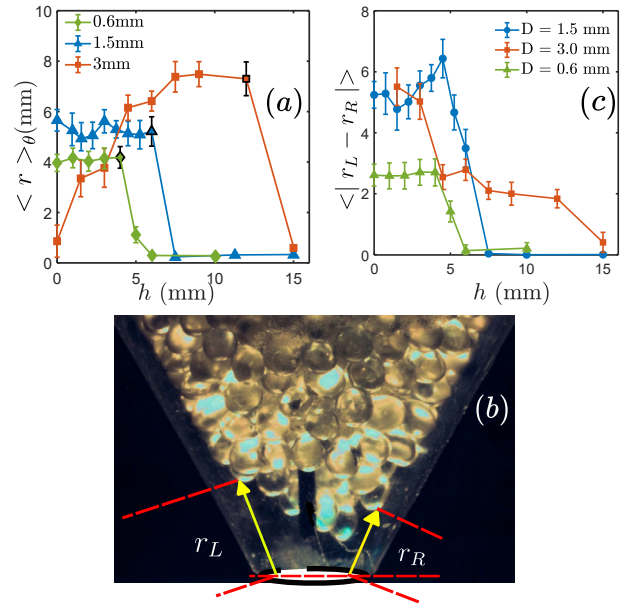


Figure 2. (a) Arch-height r (averaged over angle, θ , and different realizations) vs height h . The black color marker points to h_{pk} for different rod diameters. (b) A typical image of an asymmetrical interface for 1.5 mm rod at $h = h_{pk}$. It also contains the geometric descriptors for finding the asymmetry. (c) $\langle |r_L - r_R| \rangle$ average over all realizations vs height h .

the hopper, with $L = -30^\circ$ and $R = 30^\circ$ (see Fig. 2(b)). The trend, shown in Fig. 2(c), reveals that this measure is large for $h < h_{pk}$, indicating asymmetric arches, but drops rapidly for $h > h_{pk}$, corresponding to symmetric arches. Near $h = h_{pk}$, the asymmetry measure is larger for the rod with $D = 1.5$ mm compared to the other rods. The optimal rod is also the one that supports the maximally asymmetric interface. This suggests a correspondence between the asymmetry of the interface and the efficiency of the obstacle in reducing the clogging probability.

- **Rod diameter affects arch shape** To further examine the effect of the rod on the geometry of the arch, we first symmetrize it using $r' = (r(\theta) + r(-\theta))/2$. We then plot $\langle r'(\theta) \rangle$ for different rod diameters D (see Fig. 3a, b, c). For $h > h_{pk}$, the boundary ∂B becomes flat. Additionally, a distinct kink appears in the middle of the interface, see Fig. 3 a,b,c. This kink, primarily occurring for $h < h_{pk}$ is a signature of the rod piercing the interface. In Fig. 3d we compare these profiles for all three diameters at the optimal height $h = h_{pk}$. Among the three diameters, $D = 1.5$ mm, with the sharpest kink (Fig. 3d), is the optimal diameter for penetrating the jam.

4 Conclusions:

These observations expand our understanding of the mechanism of clogging suppression by an obstacle. When the obstacle is located at the optimal position, it anchors the arch at its tip, so that the arch loses support if it slips. The obstacle modifies the shape of the arch, leading to asymmetric shapes that are likely closer to failure. An inter-

esting future direction is to investigate how arch stability in the presence of an obstacle changes with hopper angle and opening size, and assess whether similar geometrical effects exist.

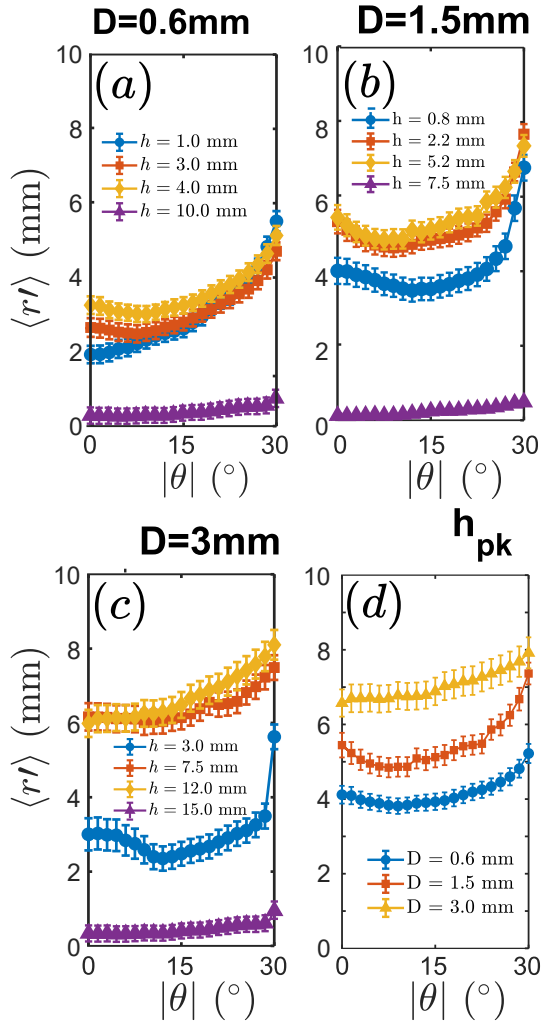


Figure 3. (a), (b), and (c) show the symmetrized projected interface profiles $\langle r' \rangle_{\theta}$ versus θ for rod diameters $D = 0.6$ mm, 1.5 mm, and 3 mm, respectively. (d) $\langle r' \rangle_{\theta}$ at $h = h_{pk}$ is shown with yellow diamonds (corresponding to panels (a), (b), and (c)) for the different rod diameters.

References

- [1] A. Sinha, J. Diodati, N. Menon, S. Tewari and S.Ghosh, Facilitating a 3D granular flow with an obstruction. *arXiv preprint arXiv:2411.11264* (2024). <https://arxiv.org/abs/2411.11264>
- [2] L. Zhu, H. Lu, M. Poletto, H. Liu, and Z. Deng, Hopper discharge of cohesive powders using pulsed airflow. *AIChE Journal* **66**(7), 16240 (2020). <https://doi.org/10.1002/aic.16240>
- [3] I. Zuriguel, A. Janda, A. Garcimartín, C. Lozano, R. Arévalo, and D. Maza, Silo clogging reduction by the presence of an obstacle. *Physical Review Letters* **107**, 278001 (2011). <https://doi.org/10.1103/PhysRevLett.107.278001>
- [4] J. Yang, D. Gong, X. Wang, Z. Wang, J. Li, B. Hu, and C. Xia, Three-dimensional clogging structures of granular spheres near hopper orifice. *Chinese Physics B* **31**(1), 014501 (2022). <https://doi.org/10.1088/1674-1056/ac3a3c>
- [5] K. To, P.-Y. Lai, and H. K. Pak, Jamming of granular flow in a two-dimensional hopper. *Physical Review Letters* **86**(1), 71 (2001). <https://doi.org/10.1103/PhysRevLett.86.71>
- [6] I. Zuriguel, A. Garcimartín, D. Maza, L. A. Pugnaloni, and J. M. Pastor, Jamming during the discharge of granular matter from a silo. *Physical Review E* **71**(5), 051303 (2005). <https://doi.org/10.1103/PhysRevE.71.051303>
- [7] J. Wang, K. Harth, D. Puzyrev, and R. Stannarius, The effect of obstacles near a silo outlet on the discharge of soft spheres. *New Journal of Physics* **24**(9), 093010 (2022). <https://doi.org/10.1088/1367-2630/ac8a60>